JOURNAL OF Materials CHEMISTRY

4-Ethoxycarbonyl-4′,5,5′-trimethyltetrathiafulvalene and its radical cation: Langmuir–Blodgett film studies, EPR spectra and the X-ray crystal structure of $(Me_3TTF\text{-}CO_2Et)_2 \cdot TCNQ$ complex

Martin R. Bryce,*[a] Adrian J. Moore,[a] Andrei S. Batsanov,[a] Judith A. K. Howard,[a] Michael C. Petty,[b] Geoffrey Williams,[b] Vincent Rotello[c] and Alejandro Cuello[c]

[a]*Department of Chemistry and Centre for Molecular Electronics, University of Durham, Durham, UK DH1 3LE. E-mail: m.r.bryce@durham.ac.uk*
[b]*School of Engineering and Centre for Molecular Electronics, University of Durham, Durham, UK DH1 3LE*
[c]*Department of Chemistry, University of Massachusetts at Amherst, Amherst, MA 01003, USA*

Received 5th July 1999, Accepted 3rd September 1999

Langmuir–Blodgett films of the title trimethyltetrathiafulvalene derivative **10** have been assembled without the need for added fatty acid: room temperature, in-plane, dc conductivity values of the films before and after doping with iodine vapour were $\sigma_{rt} = 10^{-5}$ S cm^{-1} and 10^{-1} S cm^{-1}, respectively. Over the temperature range 300–100 K the films exhibited a linear current *versus* voltage relationship, with an activation energy for conductivity $E_a = 0.11$ eV. Cyclic voltammetric data were obtained for LB films of **10** and the best response was recorded for a 2-layer film; electroactivity gradually disappeared after a few cycles, which is consistent with film desorption from the electrode. UV–vis and IR spectra of the LB films are consistent with a conjugative intramolecular charge-transfer interaction between the triMe-TTF (donor) and ester (acceptor) moieties of **10** (see structure **10′**). This increases the amphiphilic nature of **10** and is believed to play an important role in stabilising the LB film structure. Iodine doping of the LB films leads to the formation of radical cations $\mathbf{10}^{\bullet +}$, and polarised spectra show that the molecules are aligned at a high angle to the substrate surface. Simultaneous electrochemistry and EPR (SEEPR) studies provide insight into the electronic structure of the radical cation species $\mathbf{10}^{\bullet +}$ in solution; the ethoxycarbonyl group strongly polarises the spin density, and these data are supported by *ab initio* UHF and B3LYP calculations. The single crystal X-ray structure of the complex $(\mathbf{10})_2 \bullet TCNQ$ (TCNQ = tetracyano-*p*-quinodimethane) reveals a mixed $\bullet\bullet\bullet$ADDADD$\bullet\bullet\bullet$ stacking motif with a low degree of charge transfer between the D and A moieties. Analysis of the bond lengths in the donor moiety confirms a contribution from the zwitterionic structure **10′**.

Introduction

Tetrathiafulvalene (TTF) derivatives have attracted considerable interest in recent years as a number of their crystalline radical cation salts are molecular metals and superconductors.[1,2] Advances in the synthetic chemistry of the TTF system have provided access to a wide range of functionalised derivatives,[3] thereby enabling systematic studies on the structural and electronic effects of substituents. In this regard, a fruitful substitution pattern has been the attachment of one electron-withdrawing group which interacts mesomerically with the TTF ring system, *e.g.* acyl **1**,[4] ester **2**,[5] thioester **3**,[6] amide **4**[5] or thioamide **5**[7] derivatives. Intramolecular charge-transfer (ICT) in the ground state from the donor TTF unit to the acceptor substituent[3b] is clearly observed experimentally in solution studies (notably in the cyclic voltammetric and optical absorption data) and in the X-ray crystal structures of some of these derivatives, and theoretical studies have been reported for compounds **2**,[5] **4**[5] and **5**.[7]

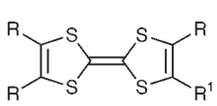

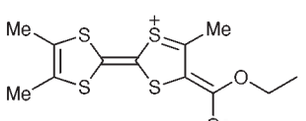

10′

1 R = H; R^1 = C(O)C$_{15}$H$_{31}$
2 R = H; R^1 = CO$_2$C$_4$H$_9$
3 R = H; R^1 = C(S)OC$_{16}$H$_{33}$
4 R = H; R^1 = C(O)NMe$_2$
5 R = H; R^1 = C(S)NHMe
6 R = H; R^1 = CO$_2$C$_6$H$_4$-N=N-C$_6$H$_5$
7 R = Me; R^1 = C(O)Ph
8 R = Me; R^1 = C(S)NHMe
9 R = Me; R^1 = CO$_2$H
10 R = Me; R^1 = CO$_2$Et

This ICT interaction is particularly important in the context of designing TTF derivatives which form stable electronically-conductive Langmuir–Blodgett (LB) films.[8] We noted that the increased hydrophilicity of the TTF head group in amphiphilic derivatives, *e.g.* compounds **1** and **3** facilitates monolayer formation on the water surface, and enables efficient build-up of multilayers on a solid substrate, in comparison with analogues in which no such mesomeric ICT is observed.[9] LB multilayers of these derivatives which display ICT generally exhibit in-plane dc room temperature conductivity values in the range $\sigma_{rt} = 10^{-3}$–10^{-1} S cm^{-1} after formation of a mixed valence state by doping with iodine vapour, although higher conductivities, $\sigma_{rt} = ca.$ 1 S cm^{-1}, have been achieved for compound **3**.[6] The beneficial effect of the ester substituent was exploited recently in the assembly of LB films of the non-

amphiphilic azobenzene-substituted TTF derivative **6**, without the need for added fatty acid.[10]

The ICT effect can be further enhanced by increasing the electron donor strength of the TTF moiety by trimethyl substitution, and derivatives **7**,[11] **8**[7] and **9**[12] have been studied in solution and in the solid state. In the present work we report on the properties of 4-ethoxycarbonyl-4′,5,5′-trimethyltetrathiafulvalene **10** and its radical cation in solution, in the solid state and in LB films. This compound was chosen for study as the mesomeric ICT effect discussed above is maximised by combining the strongly electron-donating trimethyl-TTF moiety with the electron-withdrawing ester functionality (see structure **10′**): polar trimethyl-TTF derivatives have not been explored previously as LB film-forming materials. The ethyl substituent in **10** replaces the 'traditional' long hydrophobic alkyl tail of amphiphilic LB film forming materials.

Results and discussion

Monolayer behaviour of 10 on the air–water interface and LB film transfer

Compound **10** formed a stable floating monolayer on the water surface of a Langmuir trough and a surface pressure *versus* molecular area isotherm was obtained (Fig. 1). This was reproducible and stable at the deposition pressure and was not affected by the time that the monolayer remained on the subphase before compression.[13] There was no evidence of collapse during compression of the monolayer up to the highest pressure measured (40 mN m^{-1}). The extrapolated limiting area (to zero pressure) is 0.25 nm^2 $molecule^{-1}$, which is slightly less than the cross-sectional area obtained from molecular modelling studies with geometry optimisation using Chem 3D for Macintosh (*ca.* 30 Å). This is a common feature of isotherms of more polar TTF derivatives[6,9] and we suspect that this is due to a very slight solubility of the compound in the subphase. Multilayers of compound **10** were deposited in Y-type manner with a transfer ratio on the upstroke of 0.9 ± 0.1; for the initial downstroke the deposition was less (*ca.* 0.8) but improved towards unity as further layers were deposited. Films of up to 50 monolayers could be deposited without the need for added fatty acid. This is especially notable as compound **10** contains no long alkyl chain. We suggest that the extra polarity imparted by the ICT interaction in **10** greatly assists film formation. Spectroscopic data (see below) provide evidence for the formation of ordered films after transfer. Compound **2** (with a lower degree of ICT, but a slightly longer alkyl tail) did not form stable monolayers under the same conditions.

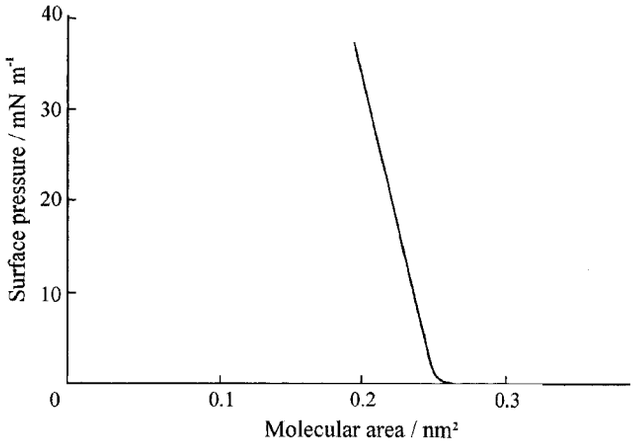

Fig. 1 Pressure *vs.* area isotherm for compound **10**.

LB Film characterisation

Conductivity studies. For all samples ohmic current–voltage characteristics were observed over the range 0–10 V. The in-plane dc conductivity values for as-deposited LB films of compound **10** were $\sigma_{rt} = ca.\ 10^{-5}$ S cm^{-1}. By varying the distance between the electrodes it was established that the effect of contact resistance was negligible. After doping with iodine vapour, which generates the radical cation species $\mathbf{10}^{\bullet +}$, the room temperature conductivity value of each sample rose to $\sigma_{rt} = 10^{-1} \pm 0.1$ S cm^{-1}. No anisotropy of conductivity was found in the film plane. This value remained constant for films stored in air for 48 h, after which time a gradual decrease in the value of the conductivity was observed. After storage for 3 weeks the value had declined to $\sigma_{rt} = ca.\ 10^{-3}$ S cm^{-1}. Over the temperature range 300–100 K the doped films exhibited a current *versus* voltage relationship, with an activation energy for conductivity $E_a = 0.11$ eV. This value is lower than that reported for most semiconducting doped LB films of TTF derivatives (typically $E_a = 0.15$–0.20 eV).[4,8] [The lowest values reported are $E_a = 0.09$ eV for iodine doped films of compound **3**,[6b] and $E_a = 0.08$ eV for films of a charge-transfer complex of a bis(ethylenedithio)-TTF derivative and tetrafluorotetracyano-*p*-quinodimethane.[14]] We also studied the effect on the conductivity values of LB films of compound **10** of electrochemical oxidation either during or after LB film deposition as described by Tieke.[8a] Both these methods afforded films with raised conductivity values of *ca.* $\sigma_{rt} = 5 \times 10^{-3}$ S cm^{-1}, clearly implying that some doping had occurred, but even after repeated experiments aimed at obtaining a mixed-valence, partially-oxidised system, this value could not be raised to that of the chemically doped films. This may be explained by two factors: (a) hindered anion diffusion within the compact multilayer assembly restricting the oxidation of the trimethyl-TTF groups; (b) instability of the films upon application of an electrochemical potential. Cyclic voltammetric (CV) data were obtained for LB films of **10** and the best response was recorded for a 2-layer film (Fig. 2a). Two redox waves expected for the TTF unit are clearly observed: in this system they are quasi-reversible. The CV curves became distorted with increasing film thickness (Fig. 2b) and electroactivity gradually disappeared after a few cycles, which is consistent with film desorption from the electrode. We consider, therefore, that (a) explains the results of attempted post-deposition electrochemical oxidation, and (b) limits the efficiency of the electrochemical doping process during film deposition. The spectroscopic data below for doped films refer to those produced by chemical doping.

Optical absorption spectra. The UV–vis spectrum of LB films of compound **10** (20 layers, as deposited) shows bands at λ_{max} 285, 320 (shoulder), 400 (shoulder) and 460 nm (Fig. 3a). The lowest energy band, which is assigned to an ICT absorption from the donor moiety (trimethyl-TTF) to the

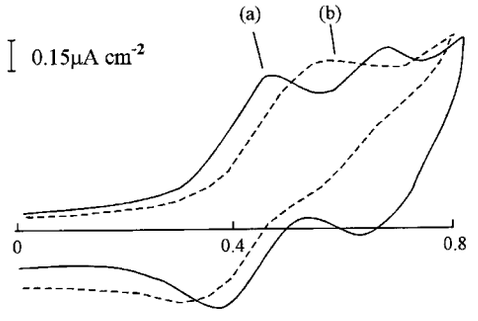

Fig. 2 Comparison of the CV response of LB films of compound **10** obtained in the same transfer experiment, in saturated KCl solution at 10 mV s^{-1}: (a) 2 layers; (b) 8 layers.

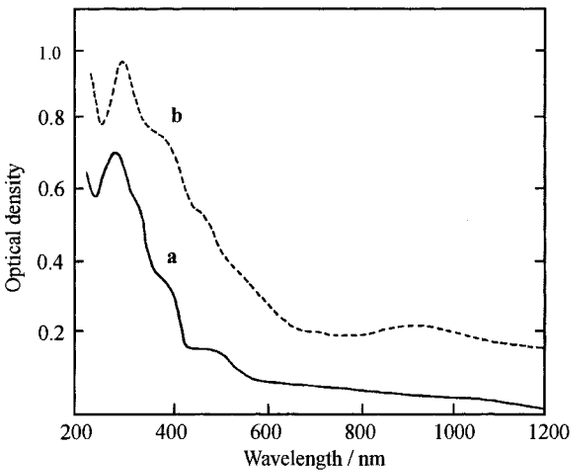

Fig. 3 UV–Visible-near IR spectra of LB films of compound **10** (20 layers): (a) before doping; (b) 1 h after iodine doping.

acceptor ethoxycarbonyl moiety, is considerably red-shifted compared to the solution spectrum (λ_{max} 415 nm in acetonitrile).[11] This could be caused by increased conjugation due to a more planar conformation of compound **10** in the compact LB film structure. The optical density of the absorption band at $\lambda_{max}=400$ nm increased linearly as a function of the number of layers (data obtained for 10, 20, 30 and 40 layers) consistent with reproducible monolayer deposition. The spectrum of the iodine-doped films shows bands at λ_{max} 300, 370 (shoulder), 450 (shoulder) and 900 nm (Fig. 3b) and there is a marked increase in the intensity of the absorption bands relative to the undoped sample, as noted previously for LB films of other TTF derivatives.[9a] The new broad band in the low energy region of the spectrum is an *inter*molecular charge-transfer band associated with the radical cation species $\mathbf{10}^{\bullet+}$, and observed previously in LB films of doped TTF derivatives.[9] Polarised spectra of the LB films after iodine doping are shown in Fig. 4. The intermolecular charge-transfer band arising from face-to-face interactions of the triMe-TTF π-systems decreases in intensity with increasing angle of incidence (measured from the substrate plane) of linearly polarised light, while the π–π* transitions of the triMe-TTF system at higher energy increase in intensity. These data provide evidence that the triMe-TTF system in the doped films is aligned at a high angle to the substrate surface.

Infrared spectroscopy. The key diagnostic features of the transmission spectra for a 16-layer sample of compound **10**, deposited on a calcium fluoride substrate, are bands at 1290 and 1705 cm^{-1} arising from the ester substituent (as observed in the spectrum of a powdered sample of **10**[11]). The spectrum obtained after doping shows new intense absorptions at 1340 and 1250 cm^{-1}, arising from vibronic conduction bands,[15] which have been analysed previously in LB films of amphiphilic TTF systems, where they have been shown to arise from a previously inactive a_g mode [ν(C=C)] becoming active.[16] The ATR and RAIRS spectra of the conducting, iodine-doped films of compound **10**, which are shown in Fig. 5, display strong dichroism. (RAIRS spectra couple only transition dipoles which are perpendicular to the substrate.) Informative differences in the spectra concern the intensities of the intermolecular charge-transfer band at 2000–5000 cm^{-1} and the vibronic conduction bands, these being strong in the ATR spectrum (Fig. 5a) but very weak in RAIRS. These data are entirely consistent with the optical absorption data discussed above, and show that conduction occurs parallel to the substrate surface, which is consistent with well-ordered stacking of the TTF rings in the LB film. It is noteworthy

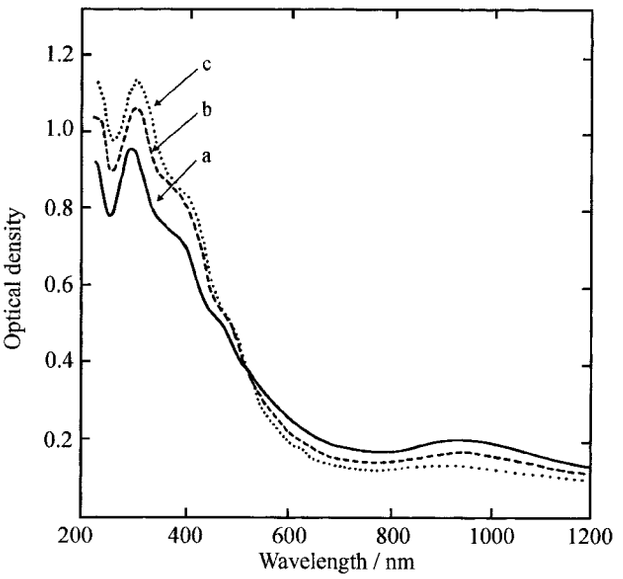

Fig. 4 UV–Visible-near IR spectra of LB films of compound **10** (20 layers) 1 h after iodine doping at different angles of incidence parallel to the plane of the substrate: (a) angle = 0°; (b) 30°; (c) 45°.

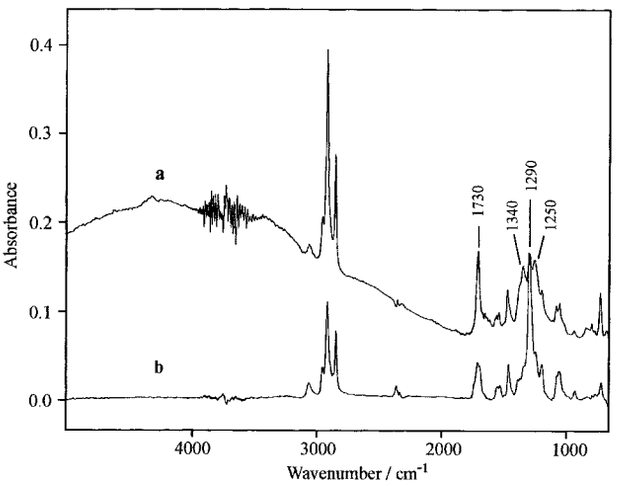

Fig. 5 Comparison of (a) ATR and (b) RAIRS spectra of LB films of compound **10** (20 layers), 1 h after iodine doping.

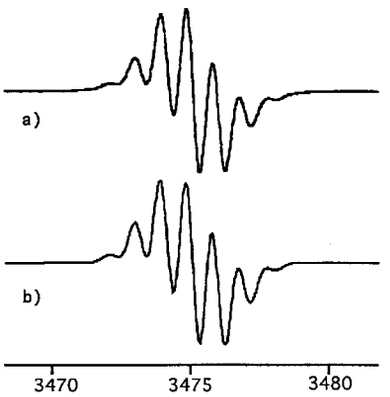

Fig. 6 SEEPR spectrum of $\mathbf{10}^{\bullet+}$ a) experimental and b) curve-fit simulation.

that the ester band at 1705 cm^{-1} shifts to 1730 cm^{-1} in the doped film, providing further evidence for a significant conjugative interaction of this substituent with the π-electrons in the triMe-TTF system.

Table 1 Experimental and calculated hyperfine coupling constants (hfcs) for $10^{\bullet+}$

Position	Experimental hfcs	Calculated hfcs[a,b]
a	0.890	1.112
b	0.890	0.825
c	0.200	0.219
d	0.160	0.188
e	<0.010	0.006

[a]B3LYP/6-31G*//UHF/3-21G*. [b]Average value of the protons at this position.

Solution EPR studies

To explore further the ICT effect in **10** and to provide insight into the electronic structure of the TTF radical cation $\mathbf{10}^{\bullet+}$, simultaneous electrochemistry and EPR (SEEPR) studies were performed in solution (Fig. 6). Hyperfine couplings (hfcs) were obtained through spectral simulation and iterative curvefitting (Table 1, r^2 for the fit = 0.997).[17] Further correlation of the experimental results with the electronic structure of $\mathbf{10}^{\bullet+}$ was obtained using *ab initio* UHF and B3LYP calculations. As shown in Table 1, very good correlations between predicted and experimental hfcs were obtained using the B3LYP/6-31G*//UHF/3-21G* protocol[18–20] after averaging of the computationally-derived hfcs at each position (Fig. 7). This correlation allows prediction of the spin density distribution of $\mathbf{10}^{\bullet+}$, a property not experimentally accessible. As shown in Fig. 7, spin density is strongly perturbed by the ethoxycarbonyl moiety, relative to tetramethyl-TTF. This distortion is more pronounced in the proximal atoms, while moderate changes are also visible in the distal ring.

Single crystal X-ray structure of $(\mathbf{10})_2 \bullet$ TCNQ

To probe the solid state structure of **10**, crystals of the charge-transfer complex $(\mathbf{10})_2 \bullet$ TCNQ were obtained and characterised by an X-ray structural study. (Attempts to obtain crystals of an iodide salt suitable for X-ray analysis, which could provide a comparison with the iodine doped LB films, were unsuccessful.) The asymmetric unit comprises one molecule of **10** in a general position and a half of a TCNQ molecule, which is situated at an inversion centre (Fig. 8). The TCNQ molecule is planar while **10** is nearly planar, except for minor boat-like folding along the S(1)···S(2) and S(3)···S(4) vectors (by 2.9 and 2.3°, respectively) and a twist of 3.7° around the C(2)–C(7) bond. The donor (**10**) and acceptor (TCNQ) molecules are parallel within 1.6° and form a mixed ···ADDADD··· stack (Fig. 9). Since the A···D interplanar separation (3.33 Å) is much smaller than the D···D separation (3.68 Å), the stack can be described as a

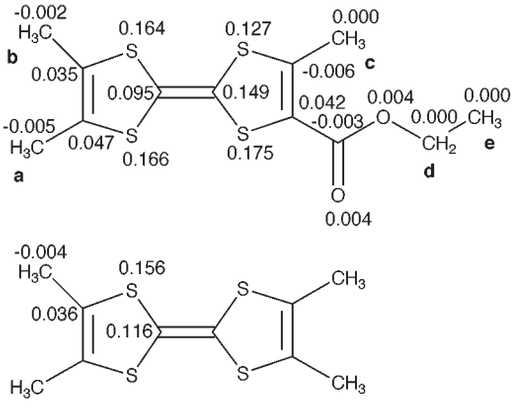

Fig. 7 Atomic spin densities for the heavy atoms (C,O,S) of $\mathbf{10}^{\bullet+}$ and tetramethyl-TTF$^{\bullet+}$.

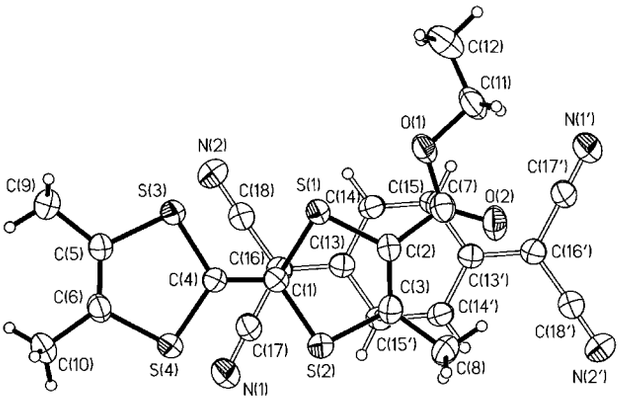

Fig. 8 Molecules of TCNQ and **10** in the structure of $(\mathbf{10})_2 \bullet$ TCNQ (50% displacement ellipsoids; primed; primed atoms are symmetrically related *via* inversion centre). Selected bond distances (Å): S(1)–C(1) 1.747(2), S(2)–C(1) 1.751(2), S(3)–C(4) 1.741(2), S(4)–C(4) 1.746(2), S(1)–C(2) 1.754(2), S(2)–C(3) 1.739(3), S(3)–C(5) 1.747(2), S(4)–C(6) 1.755(2), C(1)–C(4) 1.352(4), C(2)–C(3) 1.352(3), C(5)–C(6) 1.335(3), C(2)–C(7) 1.470(3), C(13)–C(14) 1.435(3), C(13)–C(15′) 1.432(3), C(14)–C(15) 1.346(3), C(13)–C(16) 1.384(3), C(16)–C(17) 1.427(4), C(16)–C(18) 1.430.

succession of trimers, wherein a TCNQ molecule is sandwiched between two donor molecules. The C(1) atoms of the latter are situated directly opposite the C(16) and C(16′) atoms of the TCNQ molecule at distances of 3.31 Å, much shorter than the standard van der Waals C···C contact[21] of 3.59 Å. It is known[5,22] that the HOMO of a TTF molecule is mostly localised on C(1), C(4) and the four adjacent sulfur atoms, the Mulliken atomic charge calculations[22] showing large negative charges on carbon atoms and positive charges on sulfur atoms. MO studies of **2**[22] and **10** (this work, see above) showed that an ester substituent further enhances the HOMO localisation on C(1) and C(4). On the other hand, the LUMO of a TCNQ molecule has the largest localisation (0.27) on C(16) and C(16′), the phases on which are opposite.[22] Thus the stacking mode observed in the present structure is most favourable for charge transfer.

The negative charge on a TCNQ moiety is believed[23] to correlate linearly with the differences between the C(13)–C(14) and C(13)=C(16) or between the (N)C–C(14) and C(13)=C(16) bond lengths. These differences change from 0.069 and 0.062 Å (room temperature structure corrected for libration)[24] or 0.067 and 0.064 Å (100 K structure)[25] in the neutral molecule to nil in the radical anion (−1). For the TTF•TCNQ complex,[26] this technique gives a degree of charge transfer of 0.55 to 0.60*e*, in good agreement with the value of 0.59*e* determined from neutron scattering on the superstructure.[27] In a TTF moiety, C–S bonds contract with the increase of the positive charge δ,

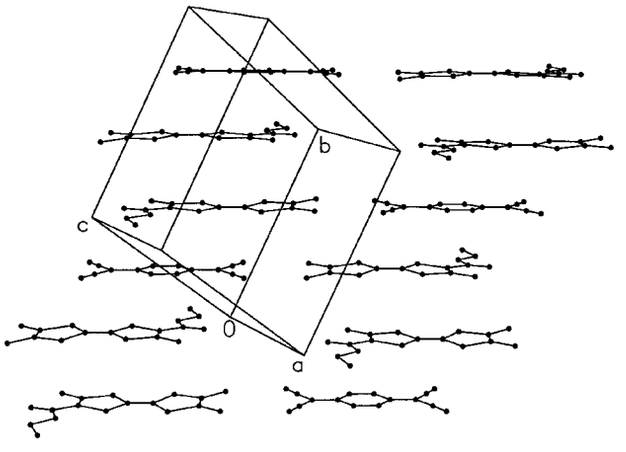

Fig. 9 Crystal packing of $(\mathbf{10})_2 \bullet$ TCNQ; H atoms are omitted.

which can be satisfactorily described[28] by a linear equation $d(\mathrm{C–S}) = 1.757 - 0.0385\ \delta$. The 'inner' C–S bonds [*i.e.* those involving C(1) and C(4)] are more reliable for these calculations, since the lengths of the 'outer' ones are strongly affected by substituents and also less accurately determined due to thermal motion.

For $(\mathbf{10})_2 \bullet$TCNQ, such estimates give a charge of -0.28 ± 0.05 for the TCNQ and of $+0.28 \pm 0.05$ for the TTF moiety, the balance probably being ICT from the TTF moiety to the ester group within **10**. In the neutral molecule of **2**, closely related to **10**, such ICT was estimated by MO calculations[5] as 0.1 to 0.2*e*. In any case, $(\mathbf{10})_2 \bullet$TCNQ exhibits a lower degree of *inter*molecular CT than TTF•TCNQ (see above), which is not surprising, as the oxidation potential of **10** ($E_1^{1/2}$ 0.40 V, *vs.* Ag/AgCl in MeCN)[11] is slightly higher than that of TTF ($E_1^{1/2}$ 0.34 V under the same conditions). It should be mentioned, however, that the crystal of TTF•TCNQ contains segregated rather than mixed stacks.

In all previously studied species (both neutral and oxidised) with a carbonyl or thiocarbonyl group attached to a TTF moiety, the C(7)=O or C(7)=S bond adopted the *cis*-orientation towards the S(1)–C(2) bond.[5,7,29,30] The conformation of the $-CO_2Et$ group in **10** differs from this by a 180° rotation around the C(2)–C(7) bond. As in other ester, carbamoyl and thiocarbamoyl derivatives of TTF, the S(2)–C(3) bond in **10** is shorter than the S(1)–C(2) by 0.015 Å (6σ), obviously due to a contribution of the zwitterionic structure **10′**.

Conclusions

The electronic distribution within the title TTF derivative **10** has been studied by a range of techniques, and the presence of a conjugative ICT interaction between the strong donor moiety (triMe-TTF) and the strong acceptor moiety (ethoxycarbonyl) has been demonstrated in solution and in Langmuir–Blodgett films. This interaction increases the amphiphilic nature of **10** and plays an important role in stabilising the LB film structure; after iodine doping LB films with in-plane dc conductivity values as high as $\sigma_{rt} = 10^{-1}$ S cm^{-1} have been obtained. This work clearly demonstrates that TTF derivatives which lack the traditional hydrophobic tails can be used for the formation of highly-conductive, well-ordered LB films.

Experimental

Synthesis

The synthesis of compound **10** has been reported previously.[11] The complex $(\mathbf{10})_2 \bullet$TCNQ was prepared as follows. Equimolar solutions of **10** and TCNQ in hot dry acetonitrile were mixed. The solution was cooled to room temperature, and slow partial evaporation afforded black crystals of the complex $(\mathbf{10})_2 \bullet$TCNQ (24% yield) which were isolated by filtration. Analysis found: C, 51.2; H, 3.9; N, 6.7; $C_{36}H_{32}N_4O_4S_8$ (2 : 1 stoichiometric complex) requires: C, 51.4; H, 3.8; N, 6.6%; σ_{rt} (2-probe, compressed pellet) 10^{-8} S cm^{-1}.

Characterisation

The Durham LB troughs were housed in a class 10 000 microelectronics clean room and have been described previously.[31] Compound **10** was spread on the surface of ultrapure water (obtained by reverse osmosis, deionisation and ultraviolet sterilisation) from CH_2Cl_2 solutions (0.1 g l^{-1}). The surface pressure *versus* molecular area isotherm was measured at 20 ± 2 °C, pH = 5.8 ± 0.2 and a compression rate *ca.* 4×10^{-3} nm^2 molecule^{-1} s^{-1}. The optimal dipping pressure was found to be 35 mN m^{-1}. LB films were deposited onto glass slides, quartz, conducting ITO glass slides (sheet resistance 300 Ω per square, from Balzers) and Au- and Ag-coated glass slides by the conventional vertical dipping technique. Unless specified otherwise, a dipping speed of 10 mm min^{-1} was employed and the first monolayer was dipped on the upstroke when the slide was immersed in the subphase before compression of the monolayer. To improve the hydrophilic properties of ITO, the slides were pretreated with saturated $Na_2Cr_2O_7$–concentrated H_2SO_4 solution for approximately 10 s and carefully washed with ultrapure water. Substrates with areas between 20 and 30 cm^2 were used for LB film transfer. After LB film deposition, the slides were cut carefully with a diamond tipped stylus to form several electrodes with contact areas between 0.1 and 0.5 cm^2. Au electrodes with a gap of about 30 μm and interdigitated Au electrodes with a gap of 15–20 μm were used for electrochemical doping of the LB films. These electrodes were produced as previously described.[10,32] Electrochemical doping during LB film transfer was achieved on a KI subphase (0.1 M) with a current of 6 μA, supplied from a Farnell Instruments current source between a moving vertical dipping Au array electrode and another Au counter electrode placed in the subphase outside the barrier. An EG&G PARC model 273 potentiostat with an Advanced Bryans *XY* recorder was used for the electrochemical experiments. Chemical doping of the LB films was carried out by exposure to iodine vapour in a sealed vessel.

Dc conductivity data were obtained in air by a standard two-contact method using silver paste contacts. By varying the distance between the electrodes, it was established that the contact resistance was negligible. The conductivity values were calculated using a monolayer thickness of 1.5 nm (estimated from molecular modelling). The conductivity normal to the film subphase was measured by using evaporated Au top contact dots (diameter 0.1 cm, slowly evaporated at a rate of about 0.5–1.0 nm min^{-1}) for films deposited on Au-coated glass slides. Optical absorption spectra of solutions were obtained using a Hitachi U-3000 spectrometer, and of LB films using a Perkin Elmer Lambda 19 spectrophotometer.

SEEPR experiments were carried out in a quartz flat cell. The platinum gauze working electrode was inserted into the flat part of the cell. The Ag-wire pseudoreference electrode was positioned directly above the working electrode in order to minimize the *iR*-drop, and the auxiliary electrode, a platinum wire spiral of large surface area, occupied the solvent reservoir above the flat section. EPR spectra were recorded on an IBM ESP 300 X-band spectrometer equipped with a TE_{104} dual cavity. TTF solutions (10^{-4} M in CH_2Cl_2, 0.1 M $Bu_4N^+ ClO_4^-$) were degassed by bubbling argon through them for 5 min and then injected into the cell, which was previously flushed with argon. Bulk electrolysis was then carried out simultaneously with signal acquisition (100 kHz field modulation, modulation amplitude 0.0522 G, SEEPR spectrum centered at 3475.50 G and 20 G sweep width) (25 kHz field modulation, modulation amplitude 0.0475 G). IR spectra were recorded on a Mattson-Sirius 100 Fourier transform spectrometer at 4 cm^{-1} resolution using our previously reported procedures.[16] Analysis of the data is based on selection rules and assignments for TTF discussed by Bozio *et al.*[15]

Crystal structure determination†

X-Ray diffraction experiment from a black pinacoidal single crystal ($0.25 \times 0.4 \times 0.4$ mm) was performed at room temperature with a SMART 1K CCD area detector. *Crystal data:* $C_{12}H_4N_4 \bullet 2C_{12}H_{14}O_2S_4$: $M = 841.14$, triclinic, space group $P\bar{1}$ (No. 2), $a = 7.686(3)$, $b = 11.454(4)$, $c = 11.617(5)$ Å, $\alpha = 76.59(2)$, $\beta = 80.25(2)$, $\gamma = 84.48(3)°$, $V = 978.8(7)$ Å^3, $Z = 1$, $D_c = 1.43$ g cm^{-3}, $F(000) = 436$, graphite-monochromated Mo-

†CCDC reference number 1145/183. See http://www.rsc.org/suppdata/jm/1999/2973 for crystallographic files in .cif format.

Kα radiation, $\bar{\lambda} = 0.71073$ Å, $\mu = 5.0\ \mathrm{cm}^{-1}$, ω scan mode, $2\theta \leqslant 46.5°$, 3745 reflections, of which 2701 unique ($R_{\mathrm{int}} = 0.019$). The structure was solved by direct methods (SHELXS-86 programs[33]) and refined by full-matrix least squares (SHELXL-93 software[34]) against F^2 of all data. All non-H atoms were refined with anisotropic displacement parameters; H atoms were refined in isotropic approximation (TCNQ), as 'riding' (CH_2) or in rigid-body model (methyl groups). The refinement of 254 variables converged at $R(F) = 0.036$ for 2495 data with $F^2 \geqslant 2\sigma(F^2)$, $wR(F^2) = 0.099$ for all data, goodness-of-fit 1.078, $\Delta\rho_{\max} = 0.23$, $\Delta\rho_{\min} = -0.20$ e Å^{-3}.

References

1 (*a*) J. R. Ferraro and J. M. Williams, *Introduction to Synthetic Electrical Conductors*, Academic Press, London, 1987; (*b*) J. M. Williams, J. R. Ferraro, R. J. Thorn, K. D. Carlson, U. Geiser, H. H. Wang, A. M. Kini and M.-H. Whangbo, *Organic Superconductors (including Fullerenes)*, Prentice Hall, New Jersey, 1992.

2 Reviews: (*a*) M. R. Bryce, *Chem. Soc. Rev.*, 1991, **20**, 355; (*b*) P. Day and M. Kurmoo, *J. Mater. Chem.*, 1997, **7**, 1291; (*c*) Y. Yamashita and M. Tomura, *J. Mater. Chem.*, 1998, **8**, 1933; (*d*) E. Coronado and C. J. Gómez-García, *Chem. Rev.*, 1998, **98**, 273.

3 Reviews: (*a*) J. Garín, *Adv. Heterocycl. Chem.*, 1995, **62**, 249; (*b*) M. R. Bryce, *Adv. Mater.*, 1999, **11**, 11.

4 A. S. Dhindsa, R. J. Ward, M. R. Bryce, Y. M. Lvov, H. S. Munro and M. C. Petty, *Synth. Met.*, 1990, **35**, 307.

5 A. S. Batsanov, M. R. Bryce, J. N. Heaton, A. J. Moore, P. J. Skabara, J. A. K. Howard, E. Ortí, P. M. Viruela and R. Viruela, *J. Mater. Chem.*, 1995, **5**, 1689.

6 (*a*) A. S. Dhindsa, J. P. Badyal, M. R. Bryce, M. C. Petty, A. J. Moore and Y. M. Lvov, *J. Chem. Soc., Chem. Commun.*, 1990, 970; (*b*) A. S. Dhindsa, Y. P. Song, J. P. Badyal, M. R. Bryce, Y. M. Lvov, M. C. Petty and J. Yarwood, *Chem. Mater.*, 1992, **4**, 724.

7 (*a*) A. S. Batsanov, M. R. Bryce, G. Cooke, J. N. Heaton and J. A. K. Howard, *J. Chem. Soc., Chem. Commun.*, 1993, 1701; (*b*) A. J. Moore, M. R. Bryce, A. S. Batsanov, J. N. Heaton, C. W. Lehmann, J. A. K. Howard, N. Robertson, A. E. Underhill and I. F. Perepichka, *J. Mater. Chem.*, 1998, **8**, 1541.

8 Reviews of conductive LB films: (*a*) B. Tieke, *Adv. Mater.*, 1991, **2**, 222; (*b*) M. R. Bryce and M. C. Petty, *Nature (London)*, 1995, **374**, 771; (*c*) T. Nakamura, in *Handbook of Organic Conductive Molecules and Polymers,* Vol. 1, Ed. H. S. Nalwa, Wiley, Chichester, 1997, Ch. 14, p. 727. Metallic conductivity has been reported for LB films of tetraalkylammonium Au(dmit)$_2$ complexes: T. Nakamura, H. Tanaka, K. Kojima, M. Matsumoto, H. Tachibana, M. Tanaka and Y. Kawabata, *Thin Solid Films*, 1989, **179**, 183; Y. F. Miura, M. Takenaga, A. Kasai, T. Nakamura, M. Matsumoto and Y. Kawabata, *Jpn. J. Appl. Phys.*, 1991, **30**, 3503.

9 (*a*) A. S. Dhindsa, G. Cooke, K. Lerstrup, K. Bechgaard, M. R. Bryce and M. C. Petty, *Chem. Mater.*, 1992, **4**, 720; (*b*) L. M. Goldenberg, R. Andreu, M. Savirón, A. J. Moore, J. Garín, M. R. Bryce and M. C. Petty, *J. Mater. Chem.*, 1995, **5**, 1593.

10 L. M. Goldenberg, M. R. Bryce, S. Wegener, M. C. Petty, J. P. Cresswell, I. K. Lednev, R. E. Hester and J. N. Moore, *J. Mater. Chem.*, 1997, **7**, 2003.

11 A. J. Moore, M. R. Bryce, A. S. Batsanov, J. C. Cole and J. A. K. Howard, *Synthesis*, 1995, 675.

12 A. Dolbecq, M. Fourmigué and P. Batail, *Bull. Soc. Chim. Fr.*, 1996, **113**, 83.

13 It has been noted that the structure of multilayer films of amphiphilic metal(dmit)$_2$ charge-transfer salts (metal = Ni, Pd, Pt) depends upon the time that the floating film is left on the subphase surface before compression. S. K. Gupta, D. M. Taylor, P. Dynarowicz, E. Barlow, C. E. A. Wainwright and A. E. Underhill, *Langmuir*, 1992, **8**, 3057; C. Pearson, A. S. Dhindsa, L. M. Goldenberg, R. A. Singh, R. Dieing, A. J. Moore, M. R. Bryce and M. C. Petty, *J. Mater. Chem.*, 1995, **5**, 1601. However, this is not usually observed with TTF derivatives.

14 J. P. Morand, R. Lapouyade, P. Delhaès, M. Vandevyver, J. Richard and A. Barraud, *Synth. Met.*, 1988, **27**, B569.

15 R. Bozio, I. Zanon, A. Girlando and C. Pecile, *J. Chem. Phys.*, 1979, **71**, 2282.

16 Y. P. Song, A. S. Dhindsa, M. R. Bryce, M. C. Petty and J. Yarwood, *Thin Solid Films*, 1992, **210/211**, 589.

17 NIEHS WinSim EPR, version 0.95, D. Duling, 1994, Laboratory of Molecular Biophysics, NIEHS, NIH, DHHS.

18 (*a*) A. Niemz and V. Rotello, *J. Am. Chem. Soc.*, 1997, **119**, 6833; (*b*) R. Batra, B. Giese, M. Spichty, G. Gescheidt and K. Houk, *J. Phys. Chem.*, 1996, **100**, 18 371.

19 Augmenting the basis set used for single point calculation to 6-31+G* did not provide better agreement with experimental values.

20 Gaussian 98, Revision A.3, M. J. Frisch, G. W. Trucks, H. B. Schlegel, G. E. Scuseria, M. A. Robb, J. R. Cheeseman, V. G. Zakrzewski, J. A. Montgomery, Jr., R. E. Stratmann, J. C. Burant, S. Dapprich, J. M. Millam, A. D. Daniels, K. N. Kudin, M. C. Strain, O. Farkas, J. Tomasi, V. Barone, M. Cossi, R. Cammi, B. Mennucci, C. Pomelli, C. Adamo, S. Clifford, J. Ochterski, G. A. Petersson, P. Y. Ayala, Q. Cui, K. Morokuma, D. K. Malick, A. D. Rabuck, K. Raghavachari, J. B. Foresman, J. Cioslowski, J. V. Ortiz, B. B. Stefanov, G. Liu, A. Liashenko, P. Piskorz, I. Komaromi, R. Gomperts, R. L. Martin, D. J. Fox, T. Keith, M. A. Al-Laham, C. Y. Peng, A. Nanayakkara, C. Gonzalez, M. Challacombe, P. M. W. Gill, B. Johnson, W. Chen, M. W. Wong, J. L. Andres, C. Gonzalez, M. Head-Gordon, E. S. Replogle, and J. A. Pople, Gaussian, Inc., Pittsburgh, PA, 1998.

21 R. S. Rowland and R. Taylor, *J. Phys. Chem.*, 1996, **100**, 7384.

22 J. P. Lowe, *J. Am. Chem. Soc.*, 1980, **102**, 1262.

23 S. Flandrois and D. Chasseau, *Acta Crystallogr., Sect. B*, 1977, **33**, 2744.

24 R. E. Long, R. A. Sparks and K. N. Trueblood, *Acta Crystallogr.*, 1965, **18**, 932.

25 E. D. Stevens and A. Syed, *Am. Cryst. Assoc. Ann. Meeting, Ser. 2*, 1984, **12**, 38.

26 T. J. Kistenmacher, T. E. Phillips and D. O. Cowan, *Acta Crystallogr., Sect. B*, 1974, **30**, 763.

27 R. Comes, S. M. Shapiro, G. Shirane, A. F. Garito and A. J. Heeger, *Phys. Rev. Lett.*, 1975, **35**, 1518.

28 D. A. Clemente and A. Marzotto, *J. Mater. Chem.*, 1996, **6**, 941.

29 M. R. Bryce, G. Cooke, A. S. Dhindsa, D. Lorcy, A. J. Moore, M. C. Petty, M. B. Hursthouse and A. I. Karaulov, *J. Chem. Soc., Chem. Commun.*, 1990, 816.

30 A. S. Batsanov, M. R. Bryce, G. Cooke, A. S. Dhindsa, J. N. Heaton, J. A. K. Howard, A. J. Moore and M. C. Petty, *Chem. Mater.*, 1994, **6**, 1419.

31 C. A. Jones, M. C. Petty, G. G. Roberts, G. Davies, J. Yarwood, N. M. Ratcliffe and J. W. Barton, *Thin Solid Films*, 1987, **155**, 187.

32 L. M. Goldenberg, C. Pearson, M. R. Bryce and M. C. Petty, *J. Mater. Chem.*, 1996, **6**, 699.

33 G. M. Sheldrick, *Acta Crystallogr., Sect. A*, 1990, **46**, 467.

34 G. M. Sheldrick, SHELXL-93, Program for the refinement of crystal structures, Univ. of Göttingen, Germany, 1993.

Paper 9/05364F